

GA-A27391

**A NEW PARADIGM FOR $E \times B$ VELOCITY SHEAR
SUPPRESSION OF GYRO-KINETIC TURBULENCE
AND THE MOMENTUM PINCH**

by

G.M. STAEBLER, R.E. WALTZ, J.E. KINSEY, and W.M. SOLOMON

SEPTEMBER 2012



DISCLAIMER

This report was prepared as an account of work sponsored by an agency of the United States Government. Neither the United States Government nor any agency thereof, nor any of their employees, makes any warranty, express or implied, or assumes any legal liability or responsibility for the accuracy, completeness, or usefulness of any information, apparatus, product, or process disclosed, or represents that its use would not infringe privately owned rights. Reference herein to any specific commercial product, process, or service by trade name, trademark, manufacturer, or otherwise, does not necessarily constitute or imply its endorsement, recommendation, or favoring by the United States Government or any agency thereof. The views and opinions of authors expressed herein do not necessarily state or reflect those of the United States Government or any agency thereof.

GA-A27391

A NEW PARADIGM FOR $E \times B$ VELOCITY SHEAR SUPPRESSION OF GYRO-KINETIC TURBULENCE AND THE MOMENTUM PINCH

by
G.M. STAEBLER, R.E. WALTZ, J.E. KINSEY, and W.M. SOLOMON*

This is a preprint of a paper to be presented at the 24th IAEA
Fusion Energy Conference, October 8–12, 2012, in San Diego,
California.

*Princeton Plasma Physics Laboratory, Princeton, New Jersey, USA.

**Work supported by
the U.S. Department of Energy
under DE-FG02-95ER54309 and DE-AC02-09CH11466**

**GENERAL ATOMICS PROJECT 03726
SEPTEMBER 2012**



A New Paradigm for $E \times B$ Velocity Shear Suppression of Gyro-kinetic Turbulence and the Momentum Pinch

G.M. Staebler¹, R.E. Waltz¹, J.E. Kinsey¹, and W.M. Solomon²
e-mail: staebler@fusion.gat.com

¹General Atomics, PO Box 85608, San Diego, California 92186-5608, USA

²Princeton Plasma Physics Laboratory, Princeton, New Jersey 08543-0451, USA

e-mail: Gary.Staebler@gat.com

Abstract. Detailed studies of the nonlinear radial wavenumber spectrum of electric potential fluctuations in gyro-kinetic plasma turbulence simulations have led to a new paradigm that is capable of computing the momentum pinch. It is found that shear in the mean field $E \times B$ velocity Doppler shift (Doppler shear) suppresses turbulence by inducing a shift in the peak of the radial wavenumber spectrum and a reduction in the amplitude. An analytic model of the non-linear saturation leads to a simple formula for the spectrum that only depends on the spectral average shift in the radial wavenumber. This “spectral shift” model is the first to identify the shift in the radial wavenumber spectrum as the central mechanism by which $E \times B$ velocity shear suppresses turbulence. Using a quasilinear model of the spectral shift, the toroidal Reynolds stress due to the Doppler shear can be computed for the first time. It is shown that, when diamagnetic and neoclassical contributions to the parallel flows are included, the Doppler shear term in the Reynolds stress allows the sign of the intrinsic toroidal rotation to change. Simulation of the balanced neutral beam injection phase of a DIII-D discharge using the quasilinear model show good agreement with experiment.

1. Introduction

Suppression of turbulence by shear in the mean field $E \times B$ velocity was first proposed [1,2] as an explanation of the high confinement H-mode regime in tokamaks [3]. The theoretical mechanism was a generic paradigm of velocity shear decorrelation. The decorrelation mechanism was tested with nonlinear gyro-fluid simulations of ion temperature gradient modes with adiabatic electrons in torodial geometry [4,5]. It was found that the Doppler shear (γ_{ExB}) using the Waltz-Miller formula [6] was stabilizing but that the effect was an order of magnitude stronger than the decorrelation formulas would predict [6]. A new “quench rule” paradigm was proposed based on the turbulence simulations. For large enough Doppler shear, these ion temperature gradient (ITG) mode simulations would completely turn off or quench the turbulence. Turbulence simulations, with kinetic electrons and a higher poloidal mode number range, have shown that the turbulence does not completely quench but is reduced to a very low amplitude [7]. The quench rule has been quite successfully used in interpreting linear drift wave stability calculations and in validation of quasilinear transport models with experiments [8].

The first indication that the quench rule was incomplete was the inability to compute the Reynolds stress induced by the Doppler shear [9–11]. Both the decorrelation and quench rule models only reduce the amplitude of the turbulence intensity. A finite Reynolds stress requires breaking the “poloidal parity”. The poloidal parity of the gyro-kinetic equation [12]

refers to the combined operation of reflection in the poloidal angle and the parallel velocity phase space coordinate [13]: $\theta \rightarrow -\theta$, $v_{\parallel} \rightarrow -v_{\parallel}$. The utility of this symmetry is that, if the gyro-kinetic equation is invariant under this operation, the Reynolds stresses that produce momentum transport will be zero. This symmetry breaking results in an asymmetric radial wavenumber spectrum for the electric potential fluctuations as illustrated in Fig. 1 (blue) [14]. Also shown in Fig. 1 is the new model (red) for the spectrum that will be presented in the next section. The General Atomics standard case with Miller geometry is shown in Fig. 1. (GA-STD-M: $a/L_{n_e} = a/L_{n_i} = 1.0$, $a/L_{T_e} = a/L_{T_i} = 3.0$, $r/a = 0.5$, $R/a = 3.0$, $q=2$, $v_{ei}=0$, $\beta_e = 0$, $rdq/dr=1$, $\kappa = 1$, $d\kappa/dr = 0$, $\delta = 0$, $d\delta/dr = 0$ kinetic ions and electrons). The shift in the spectrum due to Doppler shear results in a finite spectral average radial wavenumber and finite parallel and perpendicular Reynolds stresses [11].

2. Spectral Shift Paradigm

The GYRO code [15] was used for the simulations in this paper and all cases neglect magnetic fluctuations keeping only the electric potential fluctuations. The time averaged, magnetic flux-surface averaged, amplitude of the electric potential fluctuations in gyro-kinetic units at a fixed poloidal $k_y = k_{\theta}\rho_s$ and radial $k_x = k_r\rho_s$ wavenumber is denoted $\Phi_{k_y,k_x} = \left\langle \left| e\tilde{\varphi}_{k_y,k_x}/T_e \right|^2 \right\rangle a/\rho_s$ where T_e = electron temperature, m_i = ion mass, B_0 = magnetic field unit [6], a = minor radius of plasma boundary, $c_s = \sqrt{T_e/m_i}$, $\Omega_s = eB_0/cm_i$, $\rho_s = c_s/\Omega_s$. All growth rates and shear rates will be in units of c_s/a . The shift of the peak of the GYRO spectrum and the reduction in peak amplitude in response to a finite Doppler shear are clearly seen in Fig. 1. In this section we will briefly present the motivation for the model (red) of the spectra shown in Fig. 1. Additional details can be found in Refs 14 and 16.

The spectral shape without Doppler shear is very well fit by the Lorentzian function

$$\Phi_{\text{model}} = \frac{\gamma^{\text{eff}}}{(c_y k_y^2 + c_x k_x^2)}, \text{ where } \gamma^{\text{eff}} = c_y k_y^2 \Phi_{k_y,k_x} \Big|_{k_x=0}, \quad (1)$$

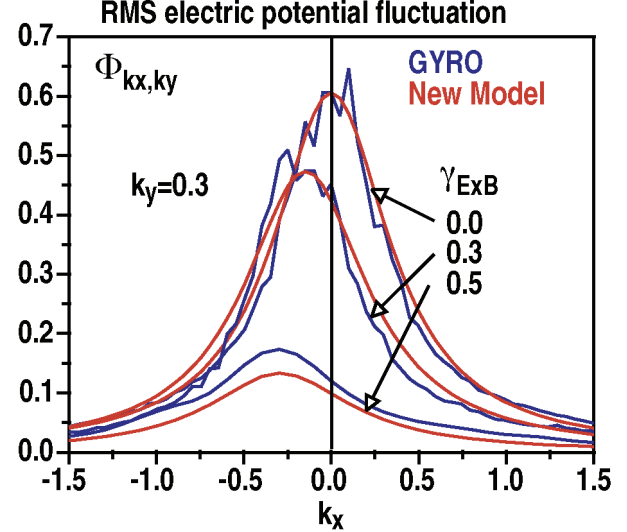


FIG. 1. Radial wavenumber spectrum of the time and flux surface averaged electric potential fluctuation amplitude Φ_k (blue) for $k_y=0.3$ and three values of the Doppler shear. Also shown are the fit model spectra (red) [Eq. (4)] [16].

The GYRO code [15] was used for the simulations in this paper and all cases neglect magnetic fluctuations keeping only the electric potential fluctuations. The time averaged, magnetic flux-surface averaged, amplitude of the electric potential fluctuations in gyro-kinetic units at a fixed poloidal $k_y = k_{\theta}\rho_s$ and radial $k_x = k_r\rho_s$ wavenumber is denoted $\Phi_{k_y,k_x} = \left\langle \left| e\tilde{\varphi}_{k_y,k_x}/T_e \right|^2 \right\rangle a/\rho_s$ where T_e = electron temperature, m_i = ion mass, B_0 = magnetic field unit [6], a = minor radius of plasma boundary, $c_s = \sqrt{T_e/m_i}$, $\Omega_s = eB_0/cm_i$, $\rho_s = c_s/\Omega_s$. All growth rates and shear rates will be in units of c_s/a . The shift of the peak of the GYRO spectrum and the reduction in peak amplitude in response to a finite Doppler shear are clearly seen in Fig. 1. In this section we will briefly present the motivation for the model (red) of the spectra shown in Fig. 1. Additional details can be found in Refs 14 and 16.

The spectral shape without Doppler shear is very well fit by the Lorentzian function

$$\Phi_{\text{model}} = \frac{\gamma^{\text{eff}}}{(c_y k_y^2 + c_x k_x^2)}, \text{ where } \gamma^{\text{eff}} = c_y k_y^2 \Phi_{k_y,k_x} \Big|_{k_x=0}, \quad (1)$$

where $c_x = 0.56c_y$ and c_y is arbitrary. The spectral average shift is defined by

$$\langle k_x \rangle = \int_{-\infty}^{\infty} dk_x \Phi_{k_y, k_x}^2 / \bar{\Phi}_{k_y}^2, \text{ where } \bar{\Phi}_{k_y}^2 = \int_{-\infty}^{\infty} dk_x \Phi_{k_y, k_x}^2 . \quad (2)$$

For the zonal flows ($k_y = 0$), the k_x spectrum is symmetric with respect to the sign of k_x and the spectral average $\langle k_x \rangle$ is zero, even for finite mean field $E \times B$ Doppler shear. This is required by the reality condition on the Fourier amplitudes of the electric potential fluctuations ($\tilde{\phi}_{k_y, k_x}^* = \tilde{\phi}_{-k_y, -k_x}$). Hence, nonlinear mode coupling to the zonal flows does not contribute to the spectral shift of the finite k_y fluctuations. Only finite k_y fluctuations contribute to the Reynolds stress. It is found that the zonal flow electric field energy is a decreasing fraction of the sum of the finite- k_y electric field energies and that the turbulence is not shut off (quenched) as was seen in adiabatic electron simulations [4,5] even for very large Doppler shear ($\gamma_{ExB}=0.8$). These are very high radial wavenumber resolution simulations [14,16] which is required in order to resolve the shift.

The model of the GYRO spectrum with Doppler shear shown in Fig. 1 is given by

$$\Phi_{fit} = \frac{\gamma^{eff} / \left[1 + (\alpha_x \langle k_x \rangle / k_y)^4 \right]}{\left[c_y k_y^2 + c_x \langle k_x \rangle^2 + c_x (k_x - \langle k_x \rangle)^2 \right]} . \quad (3)$$

It has the feature that it depends only on the spectral shift $\langle k_x \rangle$ computed from the GYRO spectra and not directly on the Doppler shear. Hence, it will be called the “spectral shift” model. The fit of the spectral shift model, Eq. (3), to the GYRO spectrum is illustrated in Fig. 1 by the red lines. The fitting coefficient in the amplitude reduction factor was determined to be $\alpha_x = 1.05$. The derivation of Eq. (3) is based on an analytic model of the nonlinear saturation of the turbulence including the Doppler shear [14]. The model shows that the Doppler shear couples to the shape of the nonlinear spectrum and is linearly destabilizing when $k_y \gamma_{ExB} \partial \Phi_{fit} / \partial k_x > 0$ and is linearly stabilizing otherwise. This linear effect initiates an asymmetric tilt of the spectrum but the nonlinear mixing re-centers the spectrum about a finite shifted radial wavenumber $\langle k_x \rangle$. The analytic model gives a linear relation between the shift and the Doppler shear $\langle k_x \rangle = -\gamma_{ExB} / \gamma^{eff}$. The actual relationship is more complicated (see below) but the form of the model, Eq. (3), expressed as a function of the shift in the simulation k_x -spectrum is robust in that the two fitting coefficients ($c_x/c_v, \alpha_x$) have been found to be approximately independent of plasma parameters. The verification of the spectral shift model, Eq. (3), for a large number of GYRO parameter scans will be presented in a future paper [16].

The new spectral shift model, Eq. (3), can be implemented in a quasilinear transport calculation. First the spectral average radial wave number shift of the GYRO turbulence simulations is approximately fit by the $\langle k_x \rangle_{fit} = k_y \beta_x \operatorname{Tanh} \left[k_{x_e} / (k_y \beta_x) \right]$, where

$$k_{x_e} = -k_y \left(\frac{\gamma_{ExB}}{\gamma_0} \right) \left\{ 0.36 + 0.38 \sigma_x \operatorname{Tanh} \left[\left(0.69 \sigma_x \frac{\gamma_{ExB}}{\gamma_0} \right)^6 \right] \right\}, \quad (4)$$

$\sigma_x = \operatorname{MIN}(k_y/0.3, 1)$ and $\beta_x = 2.0$. This has an increased slope at large γ_{ExB}/γ_0 . The factor $\operatorname{MIN}(k_y/0.3, 1)$ is needed in order to fit the spectral shift at low values of k_y . The ratio $\langle k_y \rangle / k_y$ saturates at large γ_{ExB}/γ_0 . An exact value for the saturation coefficient β_x is difficult to determine from the GYRO simulations, since the turbulence level is very low. Note that the linear growth rate γ_0 at $k_x=0$ is used in Eq. (4). Next, the linear growth rates and eigenfunctions are re-computed at this shifted radial wave number. The eigenfunctions are used to compute the quasilinear weights including the phase shift due to the finite k_x . Finally, the quasilinear weights are multiplied by a model for the integrated square amplitude to obtain the flux contribution from each k_y . These are then summed to compute the total flux. The Trapped Gyro-Landau Fluid (TGLF) equations [17] are a reduced 15-moment fluid model for the gyro-kinetic equation. They have been verified to be an accurate model for computing the linear eigenmodes. The integrated intensity used in the TGLF quasilinear flux calculation [18], without Doppler shear ($\bar{\Phi}_{k_y,0}^2$) is then modified by the integrated intensity of the spectral shift model, Eq. (3).

The TGLF quasilinear toroidal Reynolds stress using this spectral shift model is shown in Fig. 2. The negative stress for $\gamma_{ExB} > 0$ is a momentum pinch. The finite toroidal Reynolds stress results from the poloidal symmetry breaking of the $\langle k_x \rangle_{fit}$ in the linear eigenmodes. This agrees quite well with the GYRO stress as shown in Fig. 2. The symmetric shape of the GYRO radial wavenumber spectrum about the shifted peak results in the quasilinear stress at the shifted peak being close to the spectral average stress. The quench rule does not produce a Reynolds stress from the Doppler shear since it only reduces the intensity. Further examples including the energy and particle fluxes can be found in Refs. [14] and [16]. It is remarkable that fitting the properties of the k_x -spectrum for the electric potential from the nonlinear GYRO simulations results in such an accurate quasilinear model of the suppression of energy transport by Doppler shear.

3. Validation of Momentum Transport

The TGLF transport model has been extensively tested against data for energy

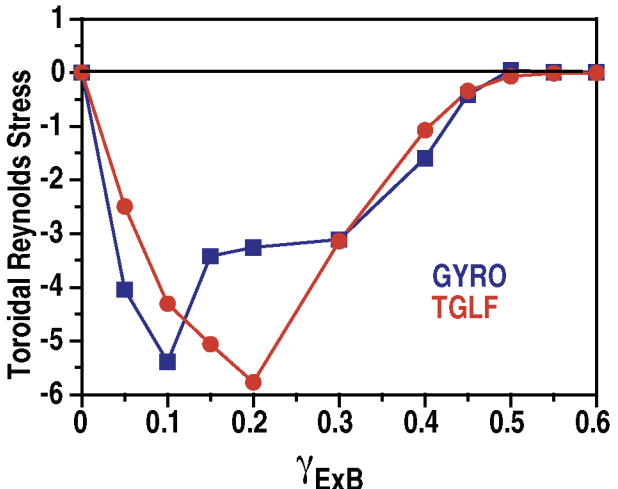


FIG. 2. Normalized toroidal Reynolds stress from GYRO simulations (blue) and the TGLF quasilinear code with the spectral shift (red) vs Doppler shear rate for the GA-STD-M case [16].

and particle transport using the measured rotation profile with the quench rule [18]. These tests have shown that including only neoclassical and gyro-kinetic turbulent transport can predict core temperature and density profiles to 17% accuracy if the boundary of the simulation domain is no larger than $r/a=0.84$. In these tests a formula for the ion neoclassical theory was used that has been found to give too large of an impurity ion contribution compared to the more accurate NEO calculation [19]. For this reason, the state of the art neoclassical code NEO will be used to compute the neoclassical transport in all channels and for electrons, main ions and the fully ionized carbon species. The carbon ion will also be included in TGLF as a kinetic species rather than only including the dilution of the main ions due to carbon (dilution approximation). The dilution approximation is acceptable for low levels of carbon impurity for energy transport since the energy flux due to carbon is proportional to the small carbon density. However, dilution becomes a poor approximation at even lower impurity densities for momentum transport since the carbon Reynolds stress is proportional to the density times the mass. In previous validation test the dilution approximation was employed.

The Reynolds stress due to parallel velocity shear and parallel flow is included in the TGLF model [16]. The large data set of Ref. 18 will need to be revisited with this more complete TGLF+NEO transport model including momentum transport and the new spectral shift model. Here only one time from a single DIII-D discharge will be studied. This discharge (125236) is from a momentum transport study [20] with an early phase with all of the neutral beam heating sources injected in the direction of the plasma current and a latter phase with the beams balanced (3500 ms) to give a near zero net torque. Due to beam orbit effects, the balanced injection case does not achieve a locally zero torque density but is slightly co-current in the center and counter current farther out. Heating during the current ramp phase was used to keep the central safety factor above the sawtooth mode boundary ($q \sim 1$) so our transport simulations will be carried out all the way to the magnetic axis. This discharge was simulated with an earlier version of TGLF before the full spectral shift model was developed [21].

The balanced beam phase (3500 ms) is shown in Fig. 3. The predicted electron density is in good agreement with the data for this case. The electron temperature prediction is too high whereas the ion temperature prediction is good. The predicted carbon rotation (neglecting diamagnetic and poloidal flows) is in surprisingly good agreement with the data. The strong peaking of the rotation near the axis is due to the small co-torque and the very low levels of transport. If the torque density in the data is artificially set to zero then the toroidal rotation is reduced to the dashed green line in Fig. 3(d). The momentum pinch effects are important in peaking the rotation profile for $r/a > 0.4$ even with the torque set to zero. The negative toroidal

rotation shear in the central core ($r/a < 0.3$) for the no-torque profile (green dashed curve) is caused by the parallel velocity driven Reynolds stress becoming positive (not a pinch). This is due to the negative magnetic shear in this region.

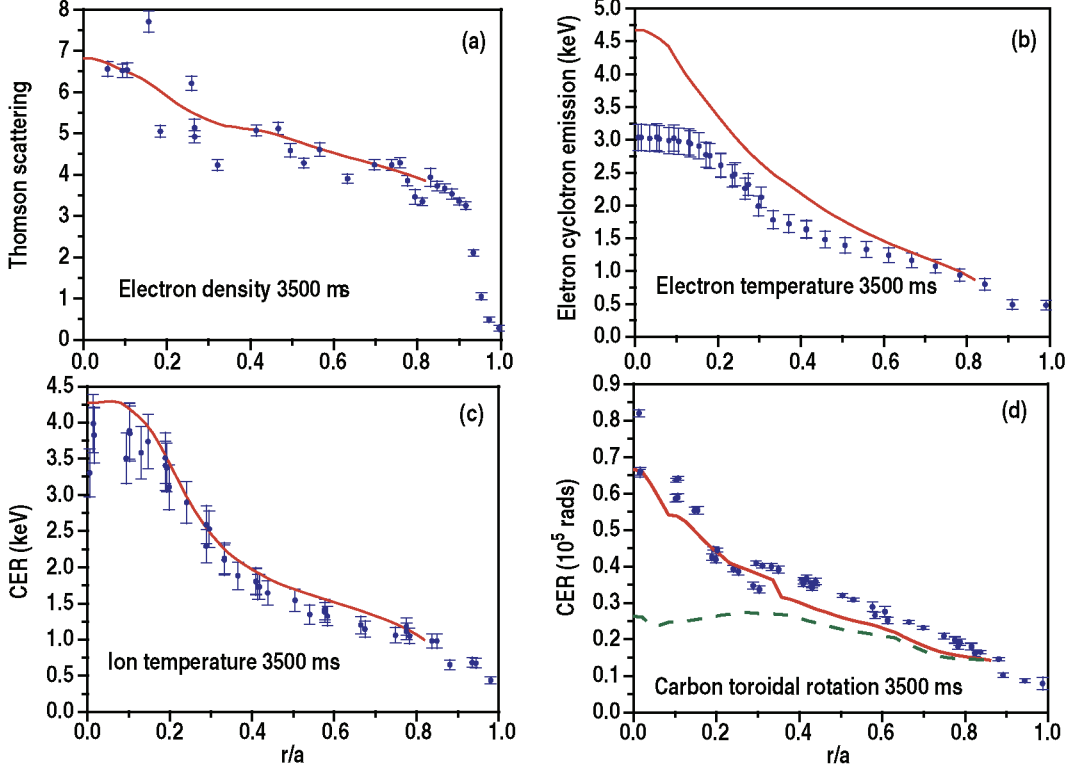


FIG. 3. TGLF + NEO multi-species simulation of the balanced NBI phase of DIII-D discharge 125236 at 3500 ms (a) electron density, (b) electron temperature, (c) ion temperature and (d) carbon angular toroidal rotation frequency for the $E \times B$ only model. The dashed green curve is the result of setting the beam torque density to zero.

Including the neoclassical poloidal and diamagnetic flows in the TGLF model does not change the predicted density or temperature profiles significantly. The predicted deuterium and carbon rotations are shown in Fig. 4. The strong peaking of the data near the axis is not matched by the predicted carbon rotation. The diamagnetic and neoclassical poloidal flows are comparable in magnitude to the $E \times B$ flow for $r/a < 0.3$ primarily due to the small poloidal magnetic field in this region. This is also where the magnetic shear is weakly negative [20] and the thermal deuterium density is hollow due to the beam ion dilution. For $r/a > 0.3$ the agreement with the measured carbon rotation in Fig. 4 is slightly better with the full model than it was without the diamagnetic and poloidal flows in Fig. 3(d). In some experiments, it has been observed that the sign of the main ion toroidal rotation can change across the profile [22] when there is no external torque. This can in principle be explained by the toroidal stress due to the Doppler shear. The toroidal stress for the main ions can be written in the form

$$\Pi_{tor} = \eta_{tor} (\gamma_p - \beta_{ExB} \gamma_{ExB} - \nu_{tor} u_p) . \quad (6)$$

The first term has parallel ion velocity shear γ_p , the second term has the $E \times B$ velocity Doppler shift shear γ_{ExB} and the third term has the momentum pinch due to the ion parallel flow u_p . If the Doppler shear term is neglected then there is no way for the parallel ion flow to change sign when there is no external torque (zero stress) since the parallel flow shear goes to zero when the flow goes to zero [23]. This changes when the Doppler shear term is included. The Doppler shear term is only from the $E \times B$ rotation whereas the ion parallel flow has $E \times B$, diamagnetic and poloidal flow contributions. Hence, the parallel flow shear can be finite even when the parallel flow vanishes and the total stress is zero due to the presence of the Doppler shear term. This analysis neglects the contribution to the Reynolds stress from up/down asymmetry of the flux surfaces [24] and from the global “profile shear” effects [25].

4. Summary

A new paradigm for the suppression of gyro-kinetic turbulence by mean field $E \times B$ velocity shear has been developed based on detailed study of the radial wave number spectrum [14]. The shear in the Doppler shift is linearly de-stabilizing on one side of the initially Lorentzian spectrum and stabilizing on the other side. This initiates an asymmetric tilt in the spectrum favoring the destabilized side but nonlinear mixing causes the spectrum to re-center (symmetrize) around a shifted maximum with reduced amplitude. A model that only depends upon the spectral average shift of the radial wave number was shown to fit the nonlinear spectrum. This “spectral shift” model has been found to be robust without change for a variety of plasma conditions [16]. The spectral shift model has been implemented in the TGLF quasilinear transport code and verified with a large number of GYRO simulations [16]. The spectral shift model improves the fit of TGLF to the nonlinear GYRO energy fluxes compared to the quench rule model, which was already quite good. In addition, the spectral shift model allows for an accurate calculation of the toroidal Reynolds stress due to the Doppler shear induced radial wave number shift.

The first validation of the spectral shift model in TGLF with data was presented in this paper. Much larger validation databases need to be predicted before any firm conclusions can be drawn as to how much of the transport is due to neoclassical and gyro-kinetic turbulent

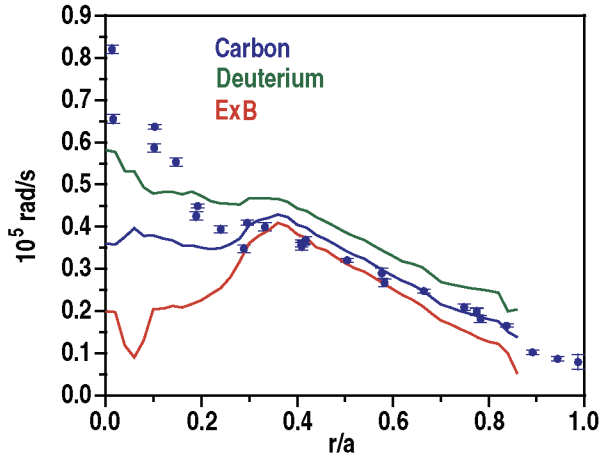


FIG. 4. TGLF + NEO simulation of the angular toroidal rotation frequency for deuterium, carbon and the $E \times B$ component for DIII-D discharge 125236 at 3500 ms including neoclassical poloidal and diamagnetic flows.

processes. This first look, at a balanced beam phase of a single DIII-D discharge, is promising. It was shown that core carbon rotation was well predicted by TGLF when the diamagnetic and poloidal flow contributions are neglected. Setting the small experimental torque to zero in the transport code showed that most of the predicted rotation for the balanced beam case for $r/a > 0.3$ was due to intrinsic turbulence processes contained in the TGLF model that produce flows even at zero Reynolds stress. It was shown that the Doppler shear contribution to the Reynolds stress makes it possible for the direction of the plasma rotation to change sign when the diamagnetic and poloidal flows are included in the parallel flow and parallel flow shear.

This work was supported by the US Department of Energy under DE-FG02-95ER54309 and DE-AC02-09CH11466.

References

- [1] SHAING, K.C. and CRUME, E.C., Phys. Rev. Lett. **63** (1989) 2369.
- [2] BIGLARI, H., et al., Phys. Fluids **B2** (1990) 1.
- [3] WAGNER, F., et al., Phys. Rev. Lett. **49** (1982) 1408.
- [4] WALTZ, R.E., et al., Phys. Plasmas **1** (1994) 2229.
- [5] WALTZ, R.E., et al., Phys. Plasmas **2** (1995) 2408.
- [6] WALTZ, R.E., et al., Phys. Plasmas **5** (1998) 1784.
- [7] KINSEY, J.E., et al., Phys. Plasmas **12** (2005) 062302.
- [8] BURRELL, K.H., Plasma Phys. Control. Fusion **36** (1994) A291, and references cited therein.
- [9] STAEBLER, G.M. and DOMINGUEZ, R.R., Nucl. Fusion **33** (1993) 77.
- [10] WALTZ, R.E., et al., Phys. Plasmas **14** (2007) 122507.
- [11] STAEBLER, G.M., et al., Phys. Plasmas **18** (2011) 056106.
- [12] ANTONSEN, T.M. and LANE, B., Phys. Fluids **23** (1980) 1205.
- [13] PEETERS, A.G. and ANGIONI, C., Phys. Plasmas **12** (2005) 072515.
- [14] STAEBLER, G.M., et al., “A New Paradigm for Suppression of Gyro-Kinetic Turbulence by Velocity Shear,” submitted to Phys. Rev. Lett. (2012).
- [15] CANDY, J. and WALTZ, R.E., J. Comp. Phys. **186** (2003) 545.
- [16] STAEBLER, G.M., et al., “Verification of the spectral shift model for ExB velocity shear,” to be submitted to Phys. Plasmas (2012).
- [17] STAEBLER, G.M., et al., Phys. Plasmas **12** (2005) 102508.
- [18] KINSEY, J.E., et al., Phys. Plasmas **15** (2008) 055908.
- [19] BELLI, E. and CANDY, J., Plasma Phys. Control. Fusion **50** (2008) 095010.
- [20] SOLOMON, W.M., et al., Plasma. Phys. Control. Fusion, **49** (2007) B313.
- [21] STAEBLER, G.M., et al., Proc. 38th EPS Conf. on Plasma Physics, Strasbourg, France, 2011, Paper O4.122.
- [22] deGRASSIE, J.S., et al., Phys. Plasmas **14** (2007) 056115.
- [23] PARRA, Felix I., et al., Phys. Plasmas **19** (2012) 056116.
- [24] CAMENEN, Y., et al., Phys. Rev. Lett. **102** (2009) 125001.
- [25] WALTZ, R.E., et al., Phys. Plasmas **18** (2011) 042504.